






## Article

# Screening of Specific and Common Pathways in Breast Cancer Cell Lines MCF-7 and MDA-MB-231 Treated with Chlorophyllides Composites

Keng-Shiang Huang <sup>1</sup>, Yi-Ting Wang <sup>2</sup>, Omkar Byadgi <sup>3</sup>, Ting-Yu Huang <sup>2</sup>, Mi-Hsueh Tai <sup>2</sup>, Jei-Fu Shaw <sup>2,\*</sup> and Chih-Hui Yang <sup>2,4,5,\*</sup>

- <sup>1</sup> The School of Chinese Medicine for Post-Baccalaureate, I-Shou University, No. 8, Yida Rd., Jiaosu Village Yanchao District, Kaohsiung City 82445, Taiwan; huangks@isu.edu.tw
  - <sup>2</sup> Department of Biological Science and Technology, I-Shou University, No. 8, Yida Rd., Jiaosu Village Yanchao District, Kaohsiung City 82445, Taiwan; teengina1220@isu.edu.tw (Y.-T.W.); z09170707@isu.edu.tw (T.-Y.H.); mihsueh@isu.edu.tw (M.-H.T.)
  - <sup>3</sup> International College, International Program in Ornamental Fish Technology and Aquatic Animal Health, National Pingtung University of Science and Technology, No. 1, Shuefu Road, Neipu, Pingtung 91201, Taiwan; omkarcof1@gmail.com
  - <sup>4</sup> Pharmacy Department, E-Da Hospital, No. 1, Yida Rd., Jiaosu Village Yanchao District, Kaohsiung City 82445, Taiwan
  - <sup>5</sup> Taiwan Instrument Research Institute, National Applied Research Laboratories, Taipei City 106214, Taiwan
- \* Correspondence: shawjf@isu.edu.tw (J.-F.S.); chyang@isu.edu.tw (C.-H.Y.); Tel.: +886-7-6151100 (ext. 7310) (J.-F.S.); +886-7-6151100 (ext. 7312) (C.-H.Y.); Fax: +886-7-6151959 (J.-F.S. & C.-H.Y.)



**Citation:** Huang, K.-S.; Wang, Y.-T.; Byadgi, O.; Huang, T.-Y.; Tai, M.-H.; Shaw, J.-F.; Yang, C.-H. Screening of Specific and Common Pathways in Breast Cancer Cell Lines MCF-7 and MDA-MB-231 Treated with Chlorophyllides Composites.

*Molecules* **2022**, *27*, 3950. <https://doi.org/10.3390/molecules27123950>

Academic Editors: Adriana Corina Hangan and Roxana Liana Lucaciu

Received: 9 May 2022

Accepted: 17 June 2022

Published: 20 June 2022

**Publisher's Note:** MDPI stays neutral with regard to jurisdictional claims in published maps and institutional affiliations.

**Abstract:** Our previous findings have shown that the chlorophyllides composites have anticancer activities to breast cancer cell lines (MCF-7 and MDA-MB-231). In the present study, microarray gene expression profiling was utilized to investigate the chlorophyllides anticancer mechanism on the breast cancer cells lines. Results showed that chlorophyllides composites induced upregulation of 43 and 56 differentially expressed genes (DEG) in MCF-7 and MDA-MB-231 cells, respectively. In both cell lines, chlorophyllides composites modulated the expression of annexin A4 (ANXA4), chemokine C-C motif receptor 1 (CCR1), stromal interaction molecule 2 (STIM2), ethanolamine kinase 1 (ETNK1) and member of RAS oncogene family (RAP2B). Further, the KEGG annotation revealed that chlorophyllides composites modulated DEGs that are associated with the endocrine system in MCF-7 cells and with the nervous system in MDA-MB-231 cells, respectively. The expression levels of 9 genes were validated by quantitative reverse transcription PCR (RT-qPCR). The expression of CCR1, STIM2, ETNK1, MAG11 and TOP2A were upregulated in both chlorophyllides composites treated-MCF-7 and MDA-MB-231 cells. The different expression of NLRC5, SLC7A7 and PKN1 provided valuable information for future investigation and development of novel cancer therapy.

**Keywords:** chlorophyllides; microarray-based detection; breast cancer; MCF-7; MDA-MB-231



**Copyright:** © 2022 by the authors. Licensee MDPI, Basel, Switzerland. This article is an open access article distributed under the terms and conditions of the Creative Commons Attribution (CC BY) license (<https://creativecommons.org/licenses/by/4.0/>).

## 1. Introduction

Breast cancer is the second most likely cause of cancer-related mortality in women [1–3]. It is evident that molecular alterations or epigenetic modifications in cancerous cells leads to the formation of the malignancies [4]. Clinical classifications of breast cancers were based on the status of estrogen receptor (ER), progesterone receptor (PR) and human epidermal growth receptor 2 (HER2) [5]. Generally, MCF-7 includes ER-positive and PR-positive breast cancer cell lines [6]. MDA-MB-231 cells are triple-negative breast cancer (TNBC), which are negative for ER, PR and HER2. Morphologically, MCF-7 and MDA-MB-231 cells are both epithelial cells that are derived from mammary gland carcinoma cells. Histologically, MCF-7 is a luminal type of breast cancer, while MDA-MB-231 is a basal type.

MCF-7 cells were effectively treated with drugs, such as tamoxifen paclitaxel, docetaxel or doxorubicin. MDA-MB-231 cells (TNBC) are found to be aggressive, prone to relapse, have high metastasis rate and poor prognosis and are insensitive to treatment [7–11].

Current treatment for breast cancer is a multi-strategy approach, including chemotherapy, surgery, radiotherapy and endocrine therapy [5,12,13]. Treatment for breast cancer (stages I–III) includes surgery and radiation therapy, with chemotherapy or other drug therapies administered before (neoadjuvant) or after (adjuvant) surgery. Chemotherapy is used mainly for downstaging, shrinking of tumors or to determine the response to therapy during early-stage breast cancer and to locally advanced breast cancer [14]. Cancer can be removed by surgery, including lumpectomy and then by whole-breast irradiation or mastectomy [15]. Whole breast irradiation is relatively acceptable, but it has inevitable acute and delayed toxic effects [16,17]. Systemic chemotherapy using cytotoxic agents or endocrine therapy are the major treatment strategy for metastatic breast cancer [12]. For example, the commonly used chemotherapy drugs—paclitaxel was diterpene (C<sub>20</sub>) formed through the condensation of four isoprene molecules [18,19]. Generally, paclitaxel was applied as a first-line (adjuvant) treatment of node-positive breast cancer [20]. For the metastatic breast cancer which has failed after combination of chemotherapy or relapse of adjuvant chemotherapy (within 6 months), paclitaxel was applied as a second line agent in breast cancer. The cytotoxic effects of paclitaxel are targeting of p53, inducing cellular apoptosis and mitotic arrest [21]. Natural compounds that are derived from plants have interesting biological activities, including antimicrobial, anti-oxidation, anti-inflammatory and cytotoxic effects [22]. The diverse range of compounds that showed potential inhibitory effects against oncogenic transcription factors in breast cancer were surveyed and reviewed, namely edomin, triterpenoids, parthenolide, vincristine, irinotecan, green tea polyphenol and several others [5,12].

Although there are several technologies for the identification of differentially expressed genes after treatment, microarray is a precise and thorough tool [23]. The advantages of microarray for gene detection are rapid, high accuracy and comprehensive detection [24,25]. Microarray technology has been used to study gene expression during the oncogenesis, metastasis or drug resistance during cancers [26–28]. Similarly, it can also be applied to the diagnosis, classification, prognosis and screening of drug targets involved in the treatment of breast cancer [29–31]. For example, microarray could be applied in cell lines with different stages of metastasis to obtain metastasis-related genes [32,33]. Further, to compare the differential expressions between different subtypes of breast cancers (e.g., MCF-7 and MDA-MB-231 cells), a large number of tumor-specific markers could be screened. Therefore, advances in microarray has made it possible and accelerated the overall study on the differentially expressed genes in breast cancer.

MDA-MB-231 cells are insensitive to conventional breast cancer treatments (e.g., chemotherapy, endocrine therapy or targeted therapy) due to drug resistance and metastasis [34–36]. The differentially expressed genes (DEGs) may be involved in signaling pathways, such as apoptosis, cell cycle and cell growth and thus have been common therapy targets in drug-resistant breast cancers. Although drugs that target important factors in signaling pathways may activate another or inhibit to resist drug effect, therapies targeting those factors have offered promising results for preventing breast cancer. Our previous studies have demonstrated that chlorophyllide composites have potential in the treatment of MDA-MB-231 cells [37,38]. However, the underlying molecular mechanisms involved have yet to be fully elucidated. Understanding the mechanisms that drive drug resistance is important to the development of novel treatment and to increase the surveillance in patients. Therefore, the main aim of this study is to characterize the effects of chlorophyllides on MCF-7 and MDA-MB-231 cells through microarray gene expression profiling. We compared the gene expression profiles among chlorophyllides composites-treated MCF-7 and MDA-MB-231 cells to exhibit the cancer-related or drug resistance-related molecular mechanism and frame a possible strategy to develop as a target of botanical drugs.

## 2. Materials and Methods

### 2.1. Materials

Ethanol and *n*-hexane were purchased from Seedchem Company Pty., Ltd. (Melbourne, Australia). 3-(4,5-dimethylthiazol-2-yl)-2,5-diphenyl tetrazolium bromide (MTT), potassium hydroxide, sodium phosphate, Triton™ X-100 and chlorophyll *a/b* standards were purchased from Sigma-Aldrich, Inc. (St. Louis, MO, USA). Sweet potato leaves were purchased from a local market in Kaohsiung, Taiwan. Human breast cancer cell lines (MCF-7 and MDA-MB-231) were purchased from the Bioresource Collection and Research Center (Food Industry Research and Development Institute, Taiwan). Dulbecco's modified Eagle's medium (DMEM) and fetal bovine serum (FBS) were obtained from Invitrogen (Carlsbad, CA, USA). TRIzol® reagent was purchased from Invitrogen Corp. (Carlsbad, CA, USA).

### 2.2. Chlorophyll Extraction and Measurement

Chlorophyll was obtained as described from the laboratory of Prof. Shaw [37]. Fresh leaf samples were washed with water and blotted. Ten grams of fresh, clean leaves were weighted and ground into powders using a mortar and pestle, with liquid nitrogen (50 mL) in the dark. Chlorophyll was extracted by immersing 1 g of leaf powder in 125 mL of ethanol. After 48 h, ethanol extract was centrifuged at  $1500\times g$  for 5 min. The chlorophyll from ethanol extracts were then sequentially extracted using *n*-hexane. After 48 h, the double extract of chlorophylls was centrifuged at  $1500\times g$  for 5 min, and purified chlorophylls from ethanol-hexane extracts were obtained. The concentrations of chlorophyll *a/b* were measured by UV-Vis spectrophotometer (BioTek Instruments, Inc., Winooski, VT, USA) for the absorbance at 649 and 665 nm, which are the major absorption peaks for chlorophyll *a* and *b*, respectively. The chlorophyll *a* and *b* contents of the leaves were calculated using previously devised equations [39].

### 2.3. Preparation of Chlorophyllides Composites by Using Chlorophyllase

Chlorophyllase was obtained as described from the laboratory of Prof. Shaw [40]. The reaction mixture contained 0.5 mg of recombinant chlorophyllase, 650  $\mu$ L of the reaction buffer (100 mM sodium phosphate (pH 7.4) and 0.24% Triton X-100) and 0.1 mL of chlorophyll extracts from the sweet potato leaves (100 mM). The reaction mixture was incubated at 37 °C for 30 min in a shaking water bath, then the enzymatic reaction was stopped by adding 1 mL of 10 mM KOH. The reaction mixture was then vortexed vigorously and centrifuged at 4000 rpm for 10 min to collect chlorophyllides composites. Chlorophyllides composites were then concentrated, and the solvents were removed by evaporation under reduced pressure at 40 °C on a rotary evaporator (IKA-Werke, Germany). The concentrated composites were processed by lyophilization, weighed and stored at  $-80$  °C for further experiments. All compounds were found to be >95% pure by HPLC analysis (Figure S1).

### 2.4. Total RNA Preparation for Sequencing

Breast cancer cell lines (MCF-7 and MDA-MB-231), cultured in DMEM supplemented with 10% FBS and maintained at 37 °C under a humidified atmosphere of 5% CO<sub>2</sub> with  $5 \times 10^4$  cells/well, were treated with 100  $\mu$ g/mL of prepared chlorophyllides composites [37,38] or DMSO (vehicle control). Cells were collected at 24 h after treatment and shipped using dry ice to Welgene Biotech. Co., Ltd., Taipei, Taiwan.

Total RNA was extracted using TRIzol® reagent according to the manufacturer's instructions [41]. The RNA quality was confirmed using the ratios A260/280 and A260/230 (Thermo fisher scientific Inc., Waltham, MA, USA). RNA concentration and integrity were analyzed by Bioanalyzer 2100 total RNA Nano series II chip (Agilent, Santa Clara, CA, USA).

### 2.5. Preparation of cDNA Library and Sequencing

RNA integrity was assessed using the RNA Nano 6000 Assay Kit on the Bioanalyzer 2100 system (Agilent Technologies, Santa Clara, CA, USA). 0.2 µg of total RNA was amplified by a Low Input Quick-Amp Labeling kit (Agilent Technologies, Santa Clara, CA, USA) and labeled with Cy3 (CyDye, Agilent Technologies, Santa Clara, CA, USA) during the in vitro transcription process. 0.6 µg of Cy3-labeled cRNA was fragmented to an average size of about 50–100 nucleotides by incubation with fragmentation buffer at 60 °C for 30 min [42].

### 2.6. Microarray Gene Expression Profiling

Microarray profiling was performed using Agilent SurePrint Microarray (Agilent Technologies, Santa Clara, CA, USA) at 65 °C for 17 h. After washing and drying by nitrogen gun blowing, microarrays were scanned with an Agilent microarray scanner (Agilent Technologies, Santa Clara, CA, USA) at 535 nm for Cy3. Scanned images were analyzed by Feature Extraction 10.7.3.1 software (Agilent Technologies, Santa Clara, CA, USA), an image analysis and normalization software was used to quantify signal and background intensity for each feature. Raw signal data was normalized by quantile normalization for differential expressed genes discovery. For functional assay, enrichment tests for gene ontology (GO) and KEGG pathway were performed for DEGs by clusterProfiler.

### 2.7. Quantitative Reverse Transcription PCR (RT-qPCR)

Validation of RNA-Seq data was performed by RT-qPCR. DNase I-treated total RNA from chlorophyllides composites-treated MCF-7 and MDA-MB-231 cells was subjected to cDNA synthesis using iScript™ cDNA synthesis kits (Bio-Rad, Hercules, CA, USA). PCR primers were designed based on the transcriptome sequences of annexin A4 (ANXA4), chemokine C-C motif receptor 1 (CCR1), stromal interaction molecule 2 (STIM2), ethanolamine kinase 1 (ETNK1) and member of RAS oncogene family (RAP2B) using Primer 2 Plus software (Table 1). GAPDH served as the internal control, and RT-qPCR was performed using iQSYBR Green Supermix (Bio-Rad Laboratories, Hercules, CA, USA), and each sample was run in triplicate. The thermal gradient feature (CFX96, Bio-Rad Laboratories) was used to determine the optimal annealing temperature for all primers. The real-time PCR program used was 95 °C for 3 min, followed by 40 cycles of 95 °C for 15 s, 58 °C for 15 s, and 72 °C for 35 s. Dissociation and melting curves of amplification products were performed and results were analyzed using the CFX Manager Software package (Bio-Rad Laboratories). The  $2^{-\Delta\Delta C_t}$  method was chosen as the calculation method [43]. The difference in the cycle threshold (Ct) value of the target gene and its housekeeping gene (GAPDH), called  $\Delta C_t$ , was calculated using the following equation:  $\Delta\Delta C_t = (\Delta C_t \text{ of chlorophyllides composites treatment or vehicle control group for the target gene at each time point}) - (\Delta C_t \text{ of the initial control})$ .

### 2.8. Statistical Analysis

Statistical comparisons were carried out by independent *t*-test using SPSS statistical software version 22.0 (SPSS Inc., Chicago, IL, USA). Values are shown as mean ± standard deviation. The acceptable level for statistical significance was  $p < 0.05$ .

**Table 1.** Primer name, sequence, target gene and product size used in the present study.

| Name     | Sequence              | Target Gene   | Product Size (bp) |
|----------|-----------------------|---------------|-------------------|
| GAPDH-F  | ATCACTGCCACCCAGA AGAC | <i>GAPDH</i>  | 460               |
| GAPDH-R  | ATGAGGTCCACCACCCTGTT  |               |                   |
| CCR1-F   | AGAAGCCGGGATGGAAACTC  | <i>CCR1</i>   | 165               |
| CCR1-R   | TTCCAACCAGGCCAATGACA  |               |                   |
| STIM2-F  | AGTCTTTGGGACTCTGCACG  | <i>STIM2</i>  | 129               |
| STIM2-R  | TGTTGCCAGCGAAAAAGTCG  |               |                   |
| ETNK1-F  | CCAAAGCATGTCTGCAACCC  | <i>ETNK1</i>  | 114               |
| ETNK1-R  | AAGCAGAAGCCTTGACCCTC  |               |                   |
| RAP2B-F  | AGCTTCCAGGACATCAAGCC  | <i>RAP2B</i>  | 190               |
| RAP2B-R  | AGGCTTTGTTTTGGCCGAC   |               |                   |
| MAGIL-F  | GCCTTGACAACCCGATCT    | <i>MAGIL</i>  | 150               |
| MAGIL-R  | GGCTTGGGTGTCCATAATAG  |               |                   |
| NLRC5-F  | ACCTTAAGCCTGTGTCCACG  | <i>NLRC5</i>  | 115               |
| NLRC5-R  | CTGTGAACCTGCCACAGCA   |               |                   |
| SLC7A7-F | CTCACTGCTTAACGGCGTGT  | <i>SLC7A7</i> | 170               |
| SLC7A7-R | CCAGTCCGCATAACAAAGG   |               |                   |
| PKN1-F   | GCCATCAAGGCTCTGAAGAA  | <i>PKN1</i>   | 136               |
| PKN1-R   | GTCTGGAAACAGCCGAAGAG  |               |                   |
| TOP2A-F  | CTTTGGCTCGATTGTTATTTC | <i>TOP2A</i>  | 142               |
| TOP2A-R  | CCCAGTACCGATTTCCTCAG  |               |                   |

### 3. Results and Discussion

#### 3.1. DEG Analysis in MCF-7 and MDA-MB-231 Cells

MCF-7 cells and MDA-MB-231 cell were subjected to chlorophyllides composites treatment, and the gene expression levels were compared. The data indicated that a total of 124 and 77 DEGs were specifically identified in MCF-7 and MDA-MB-231 cells, respectively (Figure 1A). These included 43 upregulated and 81 downregulated genes in MCF-7 and 56 upregulated and 21 downregulated genes in MDA-MB-231 cells ( $\geq 2$ -fold change (FC),  $p < 0.05$ ). To analyze the common and specific DEGs in the two cells, a Venn diagram was also performed. There were 118 specific DEGs for the chlorophyllides composites-treated MCF-7 cells and 71 specific DEGs for the chlorophyllides composites-treated MDA-MB-231 cells. We first identified the 6 overlapped genes were found between chlorophyllides composites-treated MCF-7 and MDA-MB-231 cells (Figure 1B). The results revealed that the significant differences in the chlorophyllides composites-treated MCF-7 and MDA-MB-231 cells as compared to their parental cells. Therefore, chlorophyllides composites targeted and affected the expression of DEGs, indicating that chlorophyllides composites specifically inhibited the proliferation of MCF-7 and MDA-MB-231 cells. This finding is consistent with our previous results [38]. Furthermore, a higher number of DEGs was found in MCF-7, indicating that chlorophyllides composites were more efficient in MCF-7 cells.

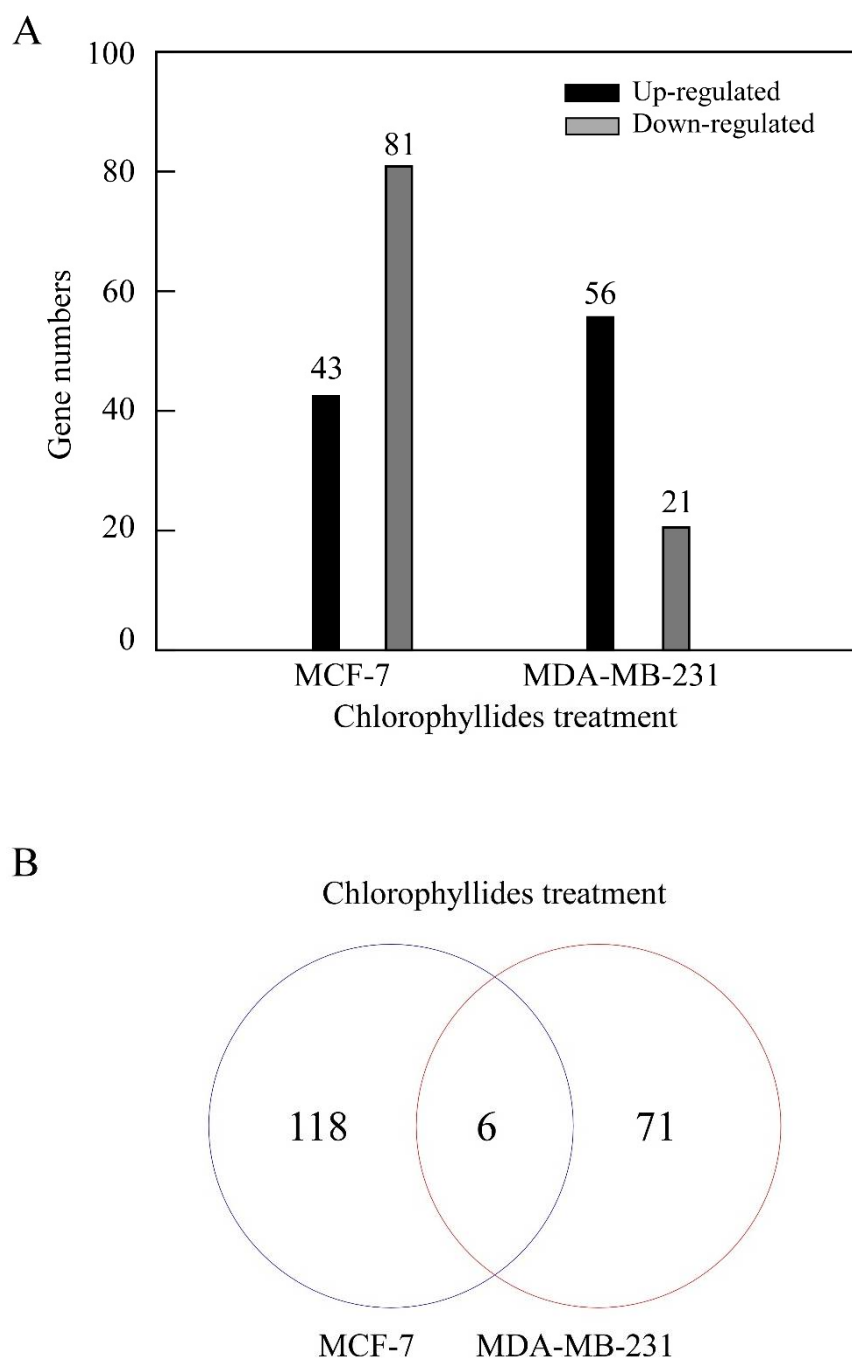


**Figure 1.** Comparisons of differentially expressed genes (DEGs) from MCF-7 and MDA-MD-231. (A) Upregulation and downregulation of DEGs in MCF-7 and MDA-MD-231 cells with chlorophyllides treatments. (B) Venn diagram of the overlapped DEGs between chlorophyllides-treated MCF-7 and MDA-MB-231 cells. The MCF-7 and MDA-MB-231 cells shared six genes of DEGs.

### 3.2. GO Annotation of Differential Expressed Genes

Comparison of gene expression levels between the MCF-7 cells, subjected to chlorophyllides composites and control cells, a total of 1383 GO terms were enriched. 29, 39 and 26 genes were clustered into three categories, namely biological process (BP), cellular component (CC) and molecular function (MF). The most enriched groups with 4 genes in MF were purine nucleoside binding and nucleoside binding. Eight groups in BP were enriched, including mesenchyme development, negative regulation of catabolic process, maintenance of location, negative regulation of cell migration, negative regulation of cell motility, nega-

tive regulation of cellular component movement, negative regulation of locomotion and muscle system process. The most enriched groups with 4 genes in CC were cell leading edge and synaptic membrane.

Comparison of gene expression levels between chlorophyllides composites-treated MDA-MB-231 cells and control cells revealed that a total of 1051 GO terms were enriched. Twenty-five, 27 and 16 genes were clustered into BP, CC, and MF. Fourteen groups in MF were enriched, such as enzyme activity, cytokine activity or receptor ligand activity. The most enriched groups with 2 genes in BP were organelle fission and response to nutrient levels. The most enriched groups in CC were tertiary granule, ficolin-1-rich granule, secretory granule membrane, postsynaptic density, asymmetric synapse, postsynaptic specialization, neuron to neuron synapse, nuclear chromatin and microtubule.

To investigate the functional roles of the DEGs, specific DEGs with chlorophyllides composites treatment were mainly functionally annotated and assigned to GO terms (Figure 2). In MCF-7 cells, specific DEGs with chlorophyllides composites treatment were assigned to 958 GO terms based on sequence homology, and a total of 21 functional groups were clustered into BP, CC and MF (Figure 2A). The unigene sequences from MF were clustered into 6 different classifications. The largest subcategory within MF was “binding”, followed by “catalytic activity”. Twenty genes and 11 genes were annotated for binding and catalytic activity out of total MF. In the CC, sequences were distributed into 3 classifications. The most represented subcategories were “cell”, followed by “cellular anatomical entity”. “Metabolic process” with 246 GO annotations was the most represented among 12 subcategories within the BP, followed by “development process” for 226 GO annotations.

In MDA-MB-231 cells, specific DEGs were annotated and shown in Figure 2B. Those DEGs with chlorophyllides composites treatment were ascribed to 590 GO terms and divided into 21 functional groups (Figure 2B). The unigene sequences from MF were clustered into 7 different classifications. The largest subcategory within MF was “catalytic activity”, followed by “binding”. In the CC, sequences were distributed into 3 classifications. The most represented subcategories were “cellular anatomical entity”, followed by “cell”. “Metabolic process” with 369 GO annotations was the most represented among 11 subcategories within the BP, followed by “cellular process” for 191 GO annotations.

It has been reported that ursolic acid, quercetin, curcumin and kaempferol are potential anti-cancer compounds in the treatment of breast cancer [44–47]. Guo et al. evaluated the anti-cancer mechanism of ursolic acid by microarray [48]. They indicated that the effects of ursolic acid were by inhibition of nuclear factor kappa-B kinase (IKK)/nuclear factor kappa-B (NF- $\kappa$ B) and serine/threonine kinase protein (RAF)/ERK pathways in MCF-7 cells [48]. Bachmeier et al. reported that curcumin inhibited the phosphorylation of the IKK in breast cancer cells [49]. In the present study, our results demonstrated that the group-biological process was enriched with chlorophyllides composites treatment, indicating that chlorophyllides composites treatment may affect the metabolism, cell communication, or development. Therefore, the functional annotations of unigenes according to the GO database provide ample numbers of candidate genes and valuable information of the biological activity of chlorophyllides composites treatment in MCF-7 and MDA-MB-231 cells.

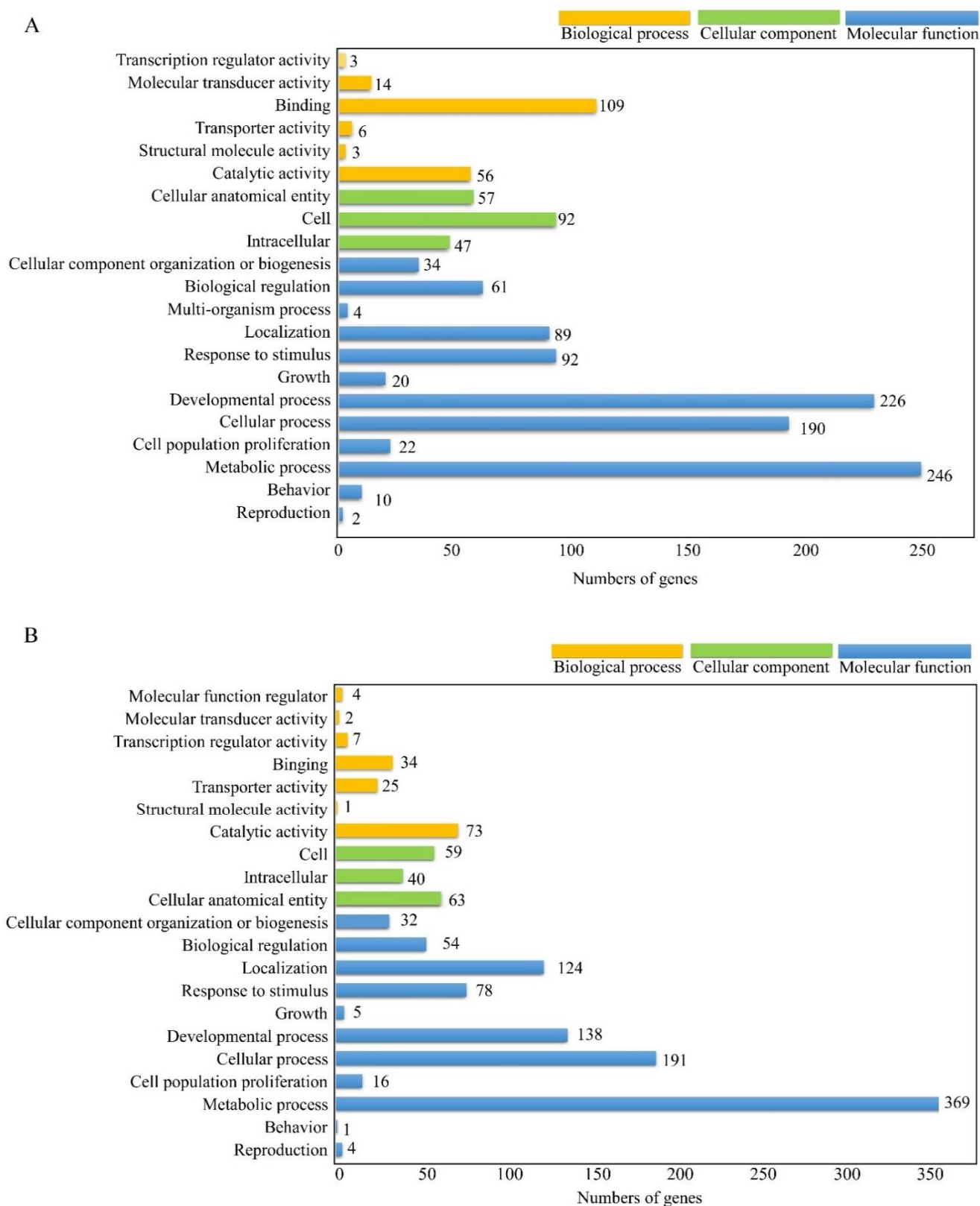


**Figure 2.** Functional distribution of GO annotation extracted from chlorophyllides composites treatments. **(A)** MCF-7 cells with chlorophyllides composites treatments. **(B)** MDA-MB-231 cells with chlorophyllides composites treatments. The results of GO enrichment analysis of DEGs were classified into three categories: molecular functions, cellular component and biological process. The *y*-axis is gene functional classification of GO, while *x*-axis is the corresponding number of genes.



### 3.3. KEGG Pathway Analysis of DEGs

Overall, specific DEGs from MCF-7 with chlorophyllides composites treatment had significant matches, which were allocated to 41 KEGG pathways classified into 6 main categories, namely metabolism, genetic information processing, environmental information processing, cellular processes, organismal systems and human diseases (Figure 3A). The highest number of genes (13 gene) categorized from KEGG analysis related to human diseases with sub-groups from viral infectious disease (3 genes), substance dependence (3 genes), cardiovascular disease (2 genes), cancer (2 genes in overview and 1 gene in specific types), neurodegenerative disease (1 gene) and endocrine and metabolic disease (1 gene). Ten genes were related to organismal systems, where the majority of the genes were categorized as endocrine system (4 genes), followed by digestive system (2 genes), sensory system (2 genes), immune system (1 gene), circulatory system (1 gene), nervous system (1 gene) and aging (1 gene). Seven genes related to environmental information processing were categorized as signal transduction (6 genes) and signaling molecules and interactions (1 gene). Six and 3 genes were related to metabolism and genetic information processing, respectively. However, no genes were categorized into cellular processes.

Moreover, DEGs from MDA-MB-231 cells with chlorophyllides composites treatment were allocated to 22 KEGG pathways (Figure 3B). The highest number of genes categorized from KEGG analysis related to organismal systems with sub-groups from the nervous or immune systems (2 genes). Seven pathways with 3 genes (RGS9, IL1B and SP11) were related to human disease. It is interesting that IL1B was categorized into 6 pathways, including of hsa05010, hsa05321, hsa05146 and hsa05152. Three genes were allotted to metabolism with subgroups of global and overview map, carbohydrate metabolism, amino acid metabolism and glycan biosynthesis and metabolism.

It has been reported that genomic profile is substantially different between MCF-7 and MDA-MB-231 cells. In the present study, we found that only 41 and 22 KEGG pathways were annotated in MCF-7 and MDA-MB-231 cells. It is worth noting that different cell lines carried specific genomic alternations, possibly due to different response to chlorophyllides composites.

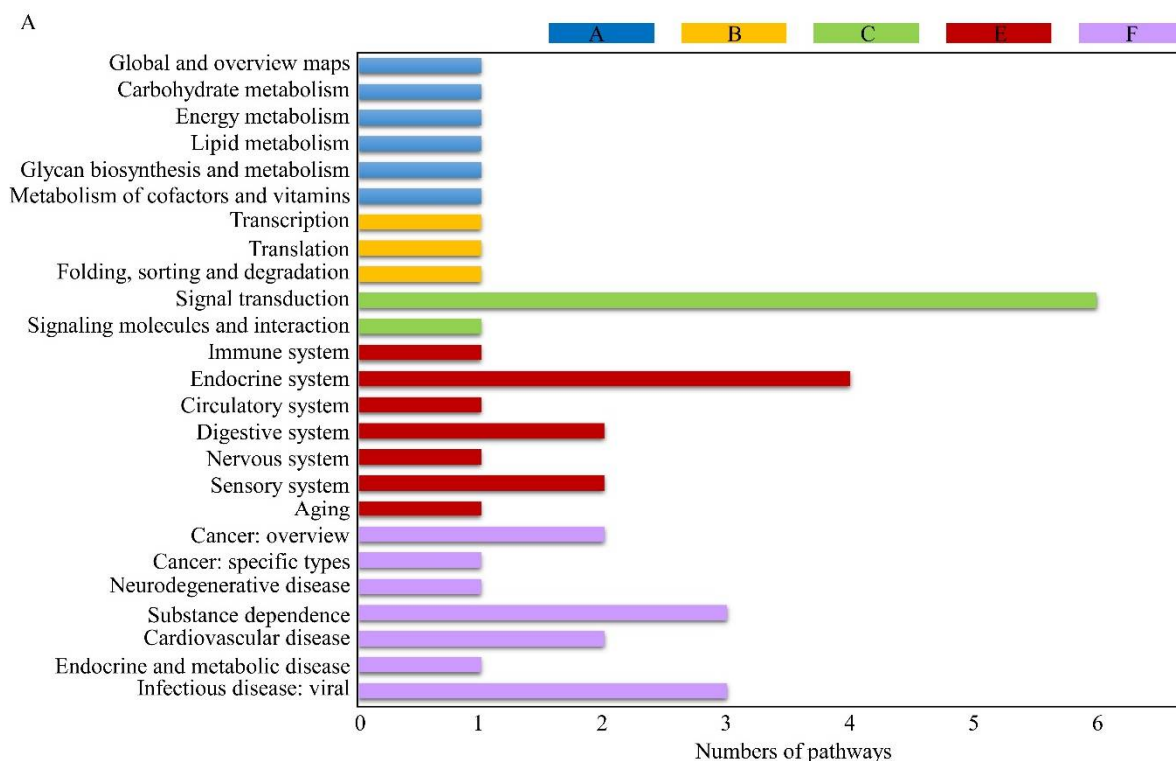
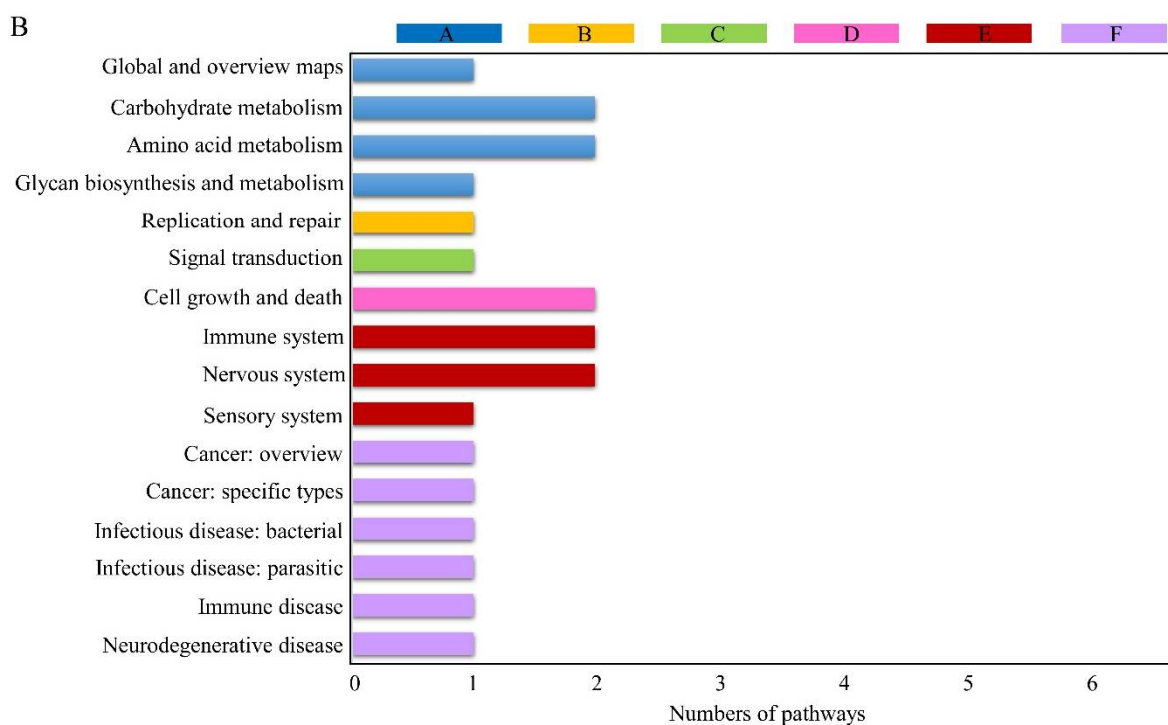


Figure 3. Cont.



**Figure 3.** KEGG (Kyoto Encyclopedia of Genes and Genomes) assembled unigenes from chlorophyllides composites treatments. (A) MCF-7 cells; (B) MDA-MB-231 cells. The results were classified into six categories: A. metabolism; B. genetic information processing; C. environmental information processing; D. cellular processes; E. organismal systems; and F. human diseases. The *y*-axis is classification of KEGG, and the *x*-axis is the corresponding numbers of pathways.  $p < 0.5$ .

### 3.4. Analysis of Common KEGG Pathways

To further identify the chlorophyllides composites relevant KEGG pathways that were common in both breast cancer cell lines, we compared the KEGG pathways that were enriched in chlorophyllides composites-treated MCF-7 and MDA-MB-231 cells (Figure 4). The top 20 common KEGG pathways were shown, including the PI3K-Akt signaling pathway, MAPK pathway, Rap1 signaling pathway or human T-cell leukemia virus 1 infection. In this study, we focused more on the underlying pathways that are related to cancer or drug resistance. Hence, the differential expression involved in cancer or drug resistance was compared between MCF-7 and MDA-MB-231 cells (Tables 2 and 3). The results revealed that 23 and 4 significantly enriched KEGG pathways related to cancer and drug resistance were identified, respectively. We observed that 90, 89 and 74 DEGs were mapped to “proteoglycans in cancer” (hsa05205), “transcriptional misregulation in cancer” (hsa05202) and “viral carcinogenesis” (hsa05203) pathways (Table 2). For the chlorophyllides composites relevant pathways in drug resistance, there were 15, 38, 42 and 45 DEGs related to “antifolate resistance” (hsa01523), “platinum drug resistance” (hsa01524), “EGFR tyrosine kinase inhibitor resistance” (hsa01521) and “endocrine resistance” (hsa01522) pathways (Table 3).

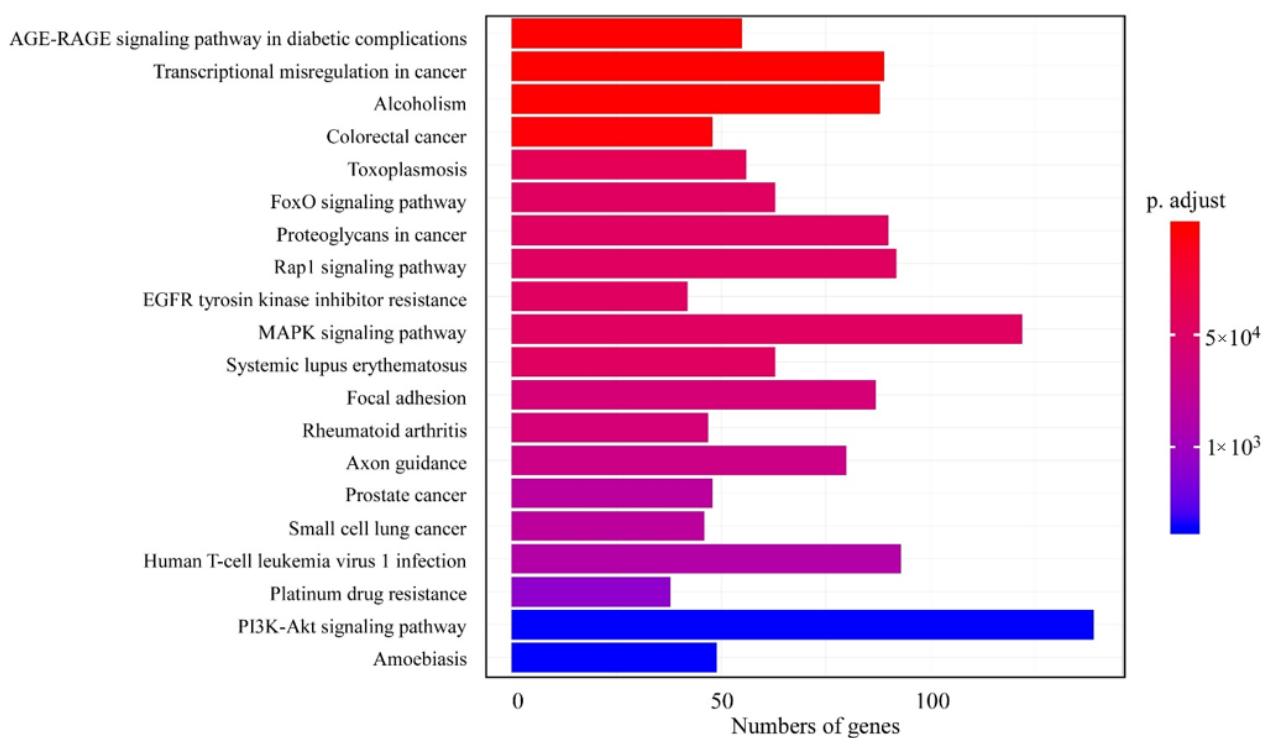


**Figure 4.** Common KEGG pathways in chlorophyllides composites-treated MCF-7 and MDA-MB-231 cells. The  $y$ -axis is classification of KEGG, and the  $x$ -axis is the corresponding number of genes.

**Table 2.** Analysis of chlorophyllides composites relevant pathway in cancers.

| Pathway ID | Pathway Description                     | Number of DEGs |      |             | All Genes with Pathway Annotation | $q$ -Value             |
|------------|---|----------------|------|-------------|-----------------------------------|------------------------|
|            |   | Up             | Down | Total DEGs  |                                   |                        |
| hsa05202   | Transcriptional misregulation in cancer | 47             | 42   | 89 (3.749%) | 186 (2.347%)                      | $1.296 \times 10^{-5}$ |
| hsa05203   | Viral carcinogenesis                    | 34             | 40   | 74 (3.117%) | 201 (2.536%)                      | 0.0428029              |
| hsa05205   | Proteoglycans in cancer                 | 35             | 55   | 90 (3.791%) | 204 (2.574%)                      | 0.0002796              |
| hsa05210   | Colorectal cancer                       | 22             | 26   | 48 (2.022%) | 86 (1.085%)                       | $2.367 \times 10^{-5}$ |
| hsa05211   | Renal cell carcinoma                    | 17             | 12   | 29 (1.222%) | 69 (0.871%)                       | 0.0433838              |
| hsa05212   | Pancreatic cancer                       | 15             | 22   | 37 (1.559%) | 69 (0.871%)                       | 0.0021288              |
| hsa05213   | Endometrial cancer                      | 13             | 14   | 27 (1.137%) | 69 (0.871%)                       | 0.0159683              |
| hsa05214   | Glioma                                  | 17             | 17   | 34 (1.432%) | 69 (0.871%)                       | 0.0118167              |
| hsa05215   | Prostate cancer                         | 25             | 23   | 48 (2.022%) | 97 (1.224%)                       | 0.0005016              |
| hsa05216   | Thyroid cancer                          | 10             | 11   | 21 (0.885%) | 37 (0.467%)                       | 0.0032991              |
| hsa05217   | Basal cell carcinoma                    | 9              | 15   | 24 (1.011%) | 63 (0.795%)                       | 0.1293504              |
| hsa05218   | Melanoma                                | 15             | 16   | 31 (1.306%) | 72 (0.909%)                       | 0.0298569              |
| hsa05219   | Bladder cancer                          | 9              | 9    | 18 (0.758%) | 41 (0.517%)                       | 0.0669118              |
| hsa05220   | Chronic myeloid leukemia                | 14             | 22   | 36 (1.516%) | 76 (0.959%)                       | 0.0045089              |

Table 2. Cont.

| Pathway ID | Pathway Description                                    | Number of DEGs |      |             | All Genes with Pathway Annotation | q-Value   |
|------------|--|----------------|------|-------------|-----------------------------------|-----------|
|            |  | Up             | Down | Total DEGs  |                                   |           |
| hsa05221   | Acute myeloid leukemia                                 | 15             | 16   | 31 (1.306%) | 67 (0.845%)                       | 0.0118167 |
| hsa05222   | Small cell lung cancer                                 | 13             | 33   | 46 (1.938%) | 92 (1.161%)                       | 0.0005016 |
| hsa05223   | Non-small cell lung cancer                             | 13             | 20   | 33 (1.390%) | 66 (0.833%)                       | 0.0029084 |
| hsa05224   | Breast cancer  | 34             | 27   | 61 (2.570%) | 147 (1.855%)                      | 0.0066776 |
| hsa05225   | Hepatocellular carcinoma                               | 32             | 40   | 72 (3.033%) | 168 (2.120%)                      | 0.0016521 |
| hsa05226   | Gastric cancer   | 30             | 28   | 58 (2.443%) | 149 (1.880%)                      | 0.0283904 |
| hsa05230   | Central carbon metabolism in cancer                    | 13             | 17   | 30 (1.264%) | 69 (0.871%)                       | 0.0286728 |
| hsa05231   | Choline metabolism in cancer                           | 20             | 16   | 36 (1.516%) | 98 (1.237%)                       | 0.1137391 |
| hsa05235   | PD-L1 expression and PD-1 checkpoint pathway in cancer | 14             | 21   | 35 (1.474%) | 89 (1.123%)                       | 0.0624114 |

Table 3. Drug resistance pathway analysis of chlorophyllides composites.

| Pathway ID | Pathway Description                       | Number of DEGs |      |             | All Genes with Pathway Annotation | q-Value   |
|------------|---|----------------|------|-------------|-----------------------------------|-----------|
|            |   | Up             | Down | Total DEGs  |                                   |           |
| hsa01521   | EGFR tyrosine kinase inhibitor resistance | 22             | 20   | 42 (1.769%) | 79 (0.997%)                       | 0.0002796 |
| hsa01522   | Endocrine resistance                      | 24             | 21   | 45 (1.896%) | 98 (1.237%)                       | 0.0032168 |
| hsa01523   | Antifolate resistance                     | 5              | 10   | 15 (0.632%) | 31 (0.391%)                       | 0.0464471 |
| hsa01524   | Platinum drug resistance                  | 15             | 23   | 38 (1.601%) | 73 (0.921%)                       | 0.0006735 |

Li et al. identified the key genes and pathways associated with metastasis of MCF-7 and MDA-MB-231 cells [50]. Further, they identified survival-correlated genes (ALOX15, COL4A6, LMB13, MTAP, PLA2G4A, TAT) and metastasis-associated genes (SNRPN, ARNT2, HDGFRP3, ERO1LB, ERLIN2, YBX2, EBF4). They also identified signaling pathways; metabolic pathways, phagosome pathway, PI3K-AKT signaling pathway, focal adhesion, ECM-receptor interaction, pancreatic secretion and human papillomavirus infection were mainly associated with metastasis. In addition, Sun et al. screened and identified common and specific genes in breast cancer subtypes basal-like, Her2, LumA, LumB and normal-like molecular subtypes [51]. The authors identified 4 common and 34 specific DEGs in different subtypes. Similar to these studies, chlorophyllides composites treatment also affected signal transduction or metabolic progress, indicating that chlorophyllides composites may act on the genes that correlated with metastasis.

### 3.5. Validation of RNA Expression by RT-qPCR

The functions of upregulated and downregulated genes are correlated with chlorophyllides composites treatment. For further understanding the role of chlorophyllides composites in breast cancers and to find potential targets for chlorophyllides composites treatment, gene expression profiles between chlorophyllides composites-treated MCF-7 cells and MDA-MB-231 cells were compared. We analyzed the microarray data sets

of upregulated and downregulated genes in MCF-7 and MDA-MB-231 cells to identify specific effects of chlorophyllides composites-induced cytotoxicity. Hierarchical clustering indicated that the DEGs were detected by chlorophyllides composites treatment between MCF-7 and MDA-MB-231 cells (Figure 5). Collectively, the levels of 52 genes were differentially expressed in MCF-7 and MDA-MB-231 cells. The expression of 16 genes was upregulated in MCF-7 cells, such as annexin A4 (ANXA4), chemokine C-C motif receptor 1 (CCR1), stromal interaction molecule 2 (STIM2), ethanolamine kinase 1 (ETNK1) and member of RAS oncogene family (RAP2B). There were 36 upregulated expressed genes in MDA-MB-231 cells, such as membrane-associated guanylate kinase WW and PDZ domain containing 1 (MAGI1), NLR family CARD domain containing 5 (NLRC5), solute carrier family 7 membrane 7 (SLC7A7), protein kinase N1 (PKN1) and DNA topoisomerase II alpha 170 kDa (TOP2A). The log<sub>2</sub> FC of CCR1, STIM2, ETNK1 and RAP2B from microarray resulted in chlorophyllides composites-treated MCF-7 cells that were 5.954, 2.783, 2.181 and 2.375, respectively. The log<sub>2</sub> FC of MAGI1, NLRC5, SLC7A7, TOP2A and PKN1 from microarray results in chlorophyllides-treated MDA-MB-231 cells were 2.307, 5.824, 22.208, 2.52 and 2.32, respectively.

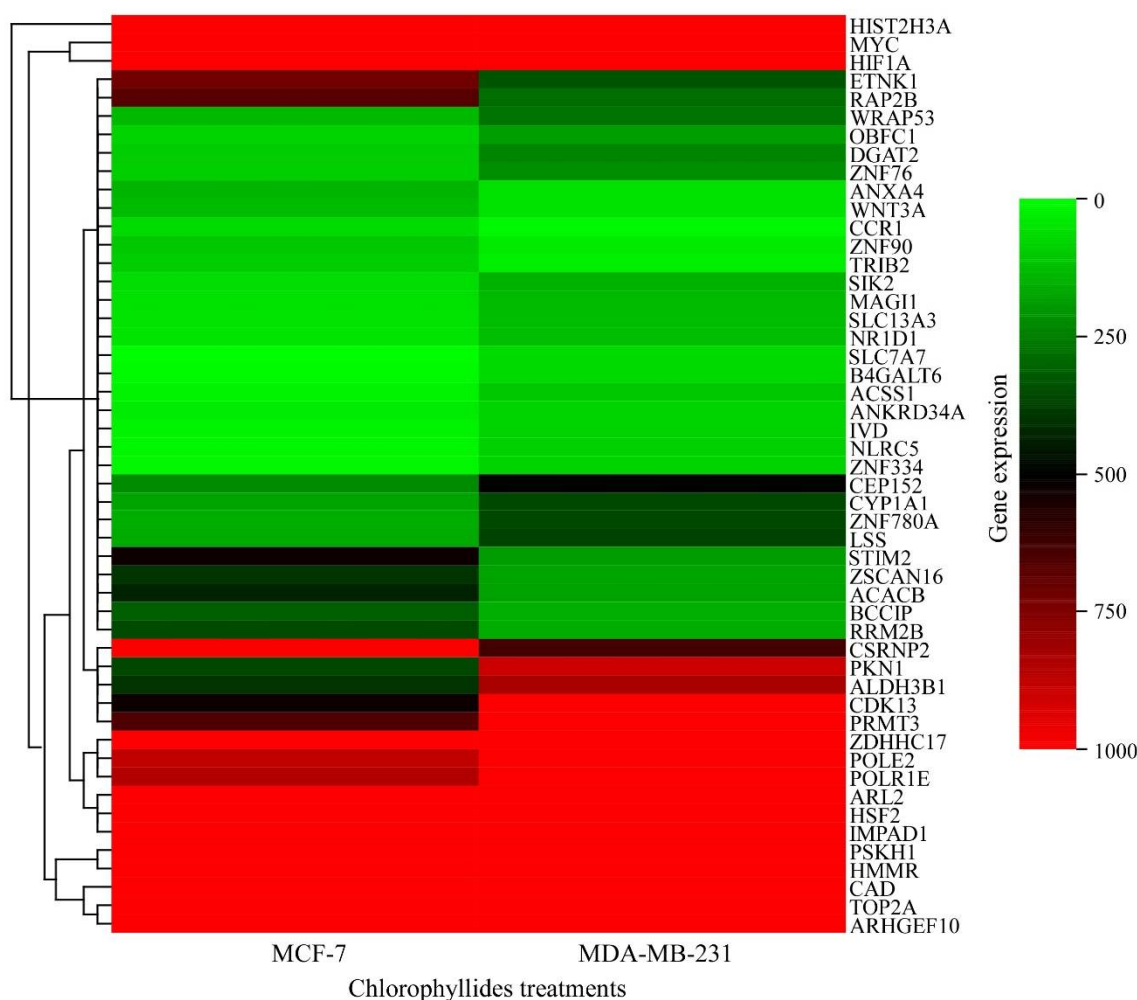


**Figure 5.** Identification of common DEGs between chlorophyllides composites-treated MCF-7 and MDA-MB-231 cells. Heat map showing the hierarchical cluster of differential expression levels between chlorophyllides composites-treated MCF-7 and MDA-MB-231 cells. The top 50 candidate genes were selected from chlorophyllide-treated MCF-7 and MDA-MB-231 cells. The color scale represents expression values; red indicates the high expression level, and the green refers to the low expression level.

To validate the expression level of CCR1, STIM2, ETNK1, RAP2B, MAG11, NLRC5, SLC7A7, TOP2A and PKN1 identified in chlorophyllides composites-treated MCF-7 and MDA-MB-231 cells, we performed RT-qPCR to evaluate their expression levels of genes as mentioned above (Figure 6). Nine randomly selected genes were detected in the chlorophyllides composites-treated MCF-7 and MDA-MB-231 cells by RT-qPCR, and the primers were listed in Table 1. The FC of CCR1, STIM2, ETNK1, MAG11 and TOP2A by RT-qPCR were 6.798, 2.687, 5.75 and 1.574, respectively. The FC of above-mentioned genes were consistent with the expression changes detected by microarray dataset. In MDA-MB-231 cells, the expression level of CCR1, STIM2, ETNK1, RAP2B, MAG11, NLRC5, SLC7A7 and TOP2A were significantly upregulated, while PKN1 was significantly downregulated. The FC of CCR1, STIM2, ETNK1, RAP2B, NLRC5, SLC7A7 and TOP2A were 10.07, 3.508, 5.95, 3.694, 5.523, 11.015 and 1.159, respectively. The FC of STIM2, RAP2B and NLRC5 were similar to the expression changes detected by RT-qPCR and microarray dataset.

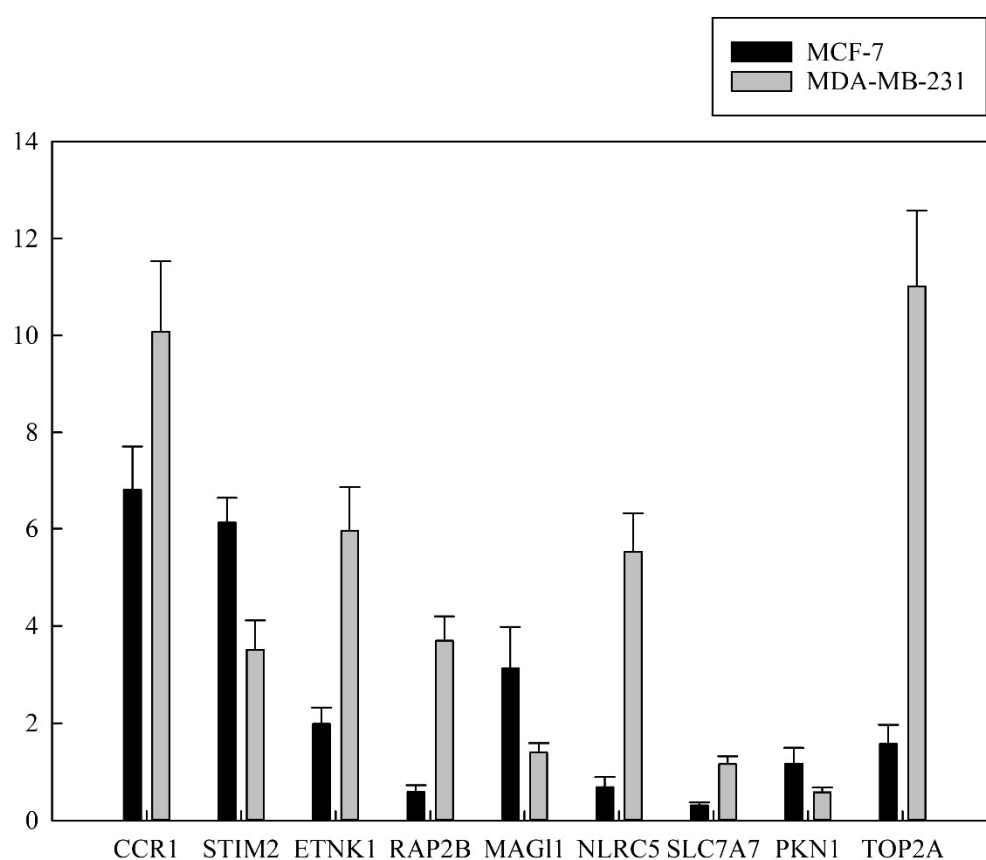


**Figure 6.** Validation of relative expression levels from RNA-seq and real-time polymerase chain reaction. Nine randomly selected differentially expressed genes (DEGs) were validated for the expression level from chlorophyllide-treated MCF-7 and MDA-MB-231 cells. Expression of target genes was normalized to GAPDH as a reference gene, and statistically significant differences from control are presented, with  $p < 0.05$ . The  $x$ -axis denotes nine genes. The  $y$ -axis refers to the relative expression level with the mean  $\pm$  standard deviation of five replicates.

The genes mentioned below were identified and mapped to the KEGG database, and their association was observed (Table 4). It has been reported that the natural products from plant sources have various biological activities, such as anti-oxidation, anti-inflammation or anti-proliferation [5]. Many of the reported anti-cancer effects of natural compounds also target cellular proteins that play important roles in signal transduction, apoptosis or cell cycle arrest [52]. By the bioinformatics analysis, we found that many DEGs were enriched in signaling and cellular process, such as CCR1, STIM2, ETNK1, RAP2B, MAG11, NLRC5, SLC7A7, PKN1 and TOP2A. Previously, we have demonstrated that purified chlorophyl-

lides composites could be a potential candidate for combination therapy to breast cancers with multiple drug resistance [38]. Therefore, we focused on several interesting factors that were differentially affected by chlorophyllides composites treatment in MCF-7 and MDA-MB-231 cells. CCR1 expression was upregulated in both MCF-7 and MDA-MB-231 cells. CCR1 belonged to the G protein-linked receptor superfamily. The expression of CCR1 has been reported on tumor cells, peripheral blood cells, immune cells and stromal cells. After the binding of CC chemokine (e.g., CCL14, CCL15, CCL16), CCR1 exhibited important roles in tumor invasion and metastasis in several cancers [53–57]. STIM2 was upregulated in both MCF-7 and MDA-MB-231 cells, and the FC in both cells was in accordance with RT-qPCR and microarray data. STIM2 is an endoplasmic reticulum-associated  $Ca^{2+}$ -sensing protein that responded to endoplasmic reticulum  $Ca^{2+}$  store depletion and transduced this cellular signal to Orai1 channel proteins [58,59]. Previous studies have demonstrated that disturbance of STIM is associated with the pathogenesis of several diseases, such as autoimmune disorders, cancer, cardiovascular disease, ageing, Alzheimer's and Huntington's diseases [60–62]. ETNK1 expression was upregulated in both MCF-7 and MDA-MB-231 cells. ETNK1 is an ethanolamine-specific kinase that catalyzes the phosphorylation of ethanolamine to generate phosphoethanolamine, which is the first step for biosynthesis of phosphatidylethanolamine. Previous studies have reported that mutations of ETNK1 may play important roles in oncogenesis [63,64]. RAP2B is a member of the Ras oncogene family that was upregulated by chlorophyllides composites in MDA-MB-231 cells. As signaling effectors of GTPase-binding protein Rap, Rap2B mediated various biological functions, including regulating the p53-mediated pro-survival function, and binding phospholipase C- $\epsilon$  and interferon- $\gamma$  that promote the development of tumors [65].

The increased levels of MAGI1 by chlorophyllides composites was observed in the MCF-7 and MDA-MB-231 cells. MAGI1 is an important protein that is transmitted from extracellular environment to intracellular signaling pathways [66,67]. It has been reported that MAGI1 functioned as a tumor suppressor in several tumors (e.g., cervical cancer, leukemia, colorectal cancer, hepatocellular carcinoma, and gastric cancer). The expression of the NLRC5 gene was upregulated in MDA-MB-231 cells, and the relative expression between MCF-7 and MDA-MB-231 cells was strongly downregulated by more than 5.523-fold. This finding is similar to the expression levels observed in microarray data (5.824 fold). NLRC5 belongs to a large protein family that is involved in the regulation of inflammatory response in tumors. Functions of NLRC5 in tumors remain as a debate [68]. NLRC5 overexpression upregulated the MHC class I-mediated antigen presentation pathway that leads to immune escape of tumor cells. In contrast, new evidence has demonstrated that NLRC5 could promote tumor malignancy [69]. Similarly, the expression of the SLC7A7 gene was upregulated in MDA-MB-231 cells, and the relative expression between MCF-7 and MDA-MB-231 cells was strongly downregulated as observed by more than 35.4-fold. The SLC7A7 gene encodes for the  $y^+$ LAT1 transporter [70,71]. The  $y^+$ LAT1 transporter was responsible for exchanging cationic amino acids with neutral amino acids and sodium at epithelial cells of the kidney and intestine. It has been reported that mutation in SLC7A7 caused a rare inherited metabolic disorder of dibasic amino acid transport-lysinuric protein intolerance.

The expression levels of the PKN1 gene in MCF-7 cells were higher in comparison to MDA-MB-231 cells. PKN1 is a member of the protein kinase C superfamily. Disruption of PKN1 kinase activity is involved in several human diseases, including cancer. A previous study has demonstrated that mitotic phosphorylation is essential for PKN1's oncogenic function [72]. It was reported that PKN1 acted as a RhoA effector that transduced androgen-responsiveness to serum response factor [73]. Overexpression of PKN1 occurred during clinical castration-recurrent prostate cancer progression, stimulated tumor growth and shortened the survival of prostate cancer xenograft. Since PKN1 belongs to the kinase family, which function as signaling proteins and are identified as successful targets for cancer treatment, it is reasonable to suggest that chlorophyllides composites may interact with PKN1 or inhibit the activity of PKN1.

**Table 4.** Differentially expressed genes (DEGs) regulate after chlorophyllides treatment between MCF-7 and MDA-MB-231 cells.

| Description  | Gene Name       | Log2 FC *  | KEGG Pathway   |
|--|-----------------|------------|--|
| Up regulation (MCF-7-chlorophyllides/MDA-MB-231-chlorophyllides)                   |                 |            |  |
| annexin A4   | <i>ANXA4</i>    | 1.3495564  | hsa04974   |
| C-C motif chemokine receptor 1   | <i>CCR1</i>     | 2.573958   | ko04060, ko04061, ko04062, ko05163, ko05167  |
| stromal interaction molecule 2   | <i>STIM2</i>    | 1.4764014  | hsa04020   |
| ethanolamine kinase 1  | <i>ETNK1</i>    | 1.1246655  | hsa00564, hsa01100   |
| RAP2B, member of RAS oncogene family   | <i>RAP2B</i>    | 1.2477774  | NA   |
| BRCA2 and CDKN1A interacting protein   | <i>BCCIP</i>    | 1.0360939  | NA   |
| ribonucleotide reductase M2 B  | <i>RRM2B</i>    | 1.1502474  | hsa00230, hsa00240, hsa00480, hsa00983, hsa01100, hsa04115   |
| cysteine-serine-rich nuclear protein 2   | <i>CSRNP2</i>   | 1.155312   | NA   |
| serine kinase H1   | <i>PSKH1</i>    | 1.1608988  | NA   |
| zinc finger and SCAN domain containing 16  | <i>ZSCAN16</i>  | 1.175633   | NA   |
| histone cluster 2, H3a   | <i>HIST2H3A</i> | 1.2060455  | hsa04613, hsa05034, hsa05131, hsa05202, hsa05322   |
| wingless-type MMTV integration site family, member 3A                              | <i>WNT3A</i>    | 1.2382799  | hsa04150, hsa04310, hsa04390, hsa04550, hsa04916, hsa04934, hsa05010, hsa05022, hsa05165, hsa05200, hsa05205, hsa05206, hsa05217, hsa05224, hsa05225, hsa05226 |
| acetyl-CoA carboxylase beta  | <i>ACACB</i>    | 1.2477973  | hsa00061, hsa00620, hsa00640, hsa01100, hsa04152, hsa04910, hsa04920, hsa04922, hsa04931   |
| zinc finger protein 90   | <i>ZNF90</i>    | 1.4318171  | hsa05168   |
| hyaluronan-mediated motility receptor  | <i>HMMR</i>     | 1.4742341  | ko04512  |
| tribbles pseudokinase 2  | <i>TRIB2</i>    | 1.5311222  | NA   |
| Down- regulation (MCF-7-chlorophyllides/MDA-MB-231-chlorophyllides)                |                 |            |  |
| membrane associated guanylate kinase, WW and PDZ domain containing 1               | <i>MAGI1</i>    | −1.2064317 | hsa04015, hsa04151, hsa04530, hsa05165   |
| NLR family, CARD domain containing 5   | <i>NLRC5</i>    | −2.5420052 | NA   |
| solute carrier family 7 (amino acid transporter light chain, y+L system), member 7 | <i>SLC7A7</i>   | −4.4729806 | hsa04974   |
| protein kinase N1  | <i>PKN1</i>     | −1.3322328 | hsa04151, hsa04621, hsa05132, hsa05135   |
| topoisomerase (DNA) II alpha 170kDa  | <i>TOP2A</i>    | −1.1590858 | hsa01524   |
| UDP-Gal:betaGlcNAc beta 1,4-galactosyltransferase, polypeptide 6                   | <i>B4GALT6</i>  | −3.2967566 | ko00600, ko01100   |
| zinc finger protein 334  | <i>ZNF334</i>   | −2.4680017 | hsa05168   |
| acyl-CoA synthetase short-chain family member 1                                    | <i>ACSS1</i>    | −2.1925126 | hsa00010, hsa00620, hsa00630, hsa00640, hsa01100, hsa01200   |
| isovaleryl-CoA dehydrogenase   | <i>IVD</i>      | −1.8816549 | ko00280, ko01100   |
| ADP-ribosylation factor-like 2   | <i>ARL2</i>     | −1.8091316 | NA   |



Table 4. Cont.

| Description  | Gene Name       | Log2 FC *  | KEGG Pathway  |
|--|-----------------|------------|---|
| Rho guanine nucleotide exchange factor 10  | <i>ARHGEF10</i> | −1.9429478 | ko04270, ko04611, ko04810, ko04928, ko05130, ko05135, ko05163, ko05200, ko05205, ko05417  |
| cyclin-dependent kinase 13   | <i>CDK13</i>    | −1.3298924 | NA  |
| diacylglycerol O-acyltransferase 2   | <i>DGAT2</i>    | −1.3269336 | ko00561, ko01100, ko04975   |
| solute carrier family 13 (sodium-dependent dicarboxylate transporter), member 3  | <i>SLC13A3</i>  | −1.3249987 | NA  |
| nuclear receptor subfamily 1, group D, member 1                                  | <i>NR1D1</i>    | −1.2920206 | ko04710   |
| zinc finger protein 76   | <i>ZNF76</i>    | −1.2438793 | hsa05168  |
| ankyrin repeat domain 34A  | <i>ANKRD34A</i> | −1.2280619 | NA  |
| salt-inducible kinase 2  | <i>SIK2</i>     | −1.2129109 | ko04922   |
| v-myc avian myelocytomatosis viral oncogene homolog                              | <i>MYC</i>      | −1.2045108 | ko04010, ko04012, ko04110, ko04151, ko04218, ko04310, ko04350, ko04390, ko04391, ko04550, ko04630, ko04919, ko05132, ko05160, ko05161, ko05163, ko05166, ko05167, ko05169, ko05200, ko05202, ko05205, ko05206, ko05207, ko05210, ko05213, ko05216, ko05219, ko05220, ko05221, ko05222, ko05224, ko05225, ko05226, ko05230 |
| zinc finger protein 780A   | <i>ZNF780A</i>  | −1.1839843 | hsa05168  |
| oligonucleotide/oligosaccharide-binding fold containing 1                        | <i>OBFC1</i>    | −1.1801386 | NA  |
| lanosterol synthase  | <i>LSS</i>      | −1.163355  | ko00100, ko01100, ko01110, ko01130  |
| zinc finger, DHHC-type containing 17   | <i>ZDHHC17</i>  | −1.1437738 | NA  |
| carbamoyl-phosphate synthetase 2, aspartate transcarbamylase, and dihydroorotase | <i>CAD</i>      | −1.1388409 | hsa00240, hsa00250, hsa01100, hsa01240  |
| centrosomal protein 152kDa   | <i>CEP152</i>   | −1.1385807 | NA  |
| hypoxia inducible factor 1, alpha subunit  | <i>HIF1A</i>    | −1.0661852 | ko04066, ko04137, ko04140, ko04212, ko04361 Axon regeneration ko04659, ko04919, ko05167, ko05200, ko05205, ko05211, ko05230, ko05231, ko05235   |
| aldehyde dehydrogenase 3 family, member B1                                       | <i>ALDH3B1</i>  | −1.063386  | hsa00010, hsa00340, hsa00350, hsa00360, hsa00410, hsa00980, hsa00982, hsa01100  |
| polymerase (DNA directed), epsilon 2, accessory subunit                          | <i>POLE2</i>    | −1.0376518 | ko03030, ko03410, ko03420   |
| arginine methyltransferase 3   | <i>PRMT3</i>    | −1.0357205 | NA  |
| polymerase (RNA) I polypeptide E, 53kDa  | <i>POLR1E</i>   | −1.0155994 | ko03020   |
| cytochrome P450, family 1, subfamily A, polypeptide 1                            | <i>CYP1A1</i>   | −1.0129887 | ko00140, ko00380, ko00830, ko00980, ko01100, ko04913, ko05204   |
| WD repeat containing, antisense to TP53  | <i>WRAP53</i>   | −1.0114268 | NA  |
| heat shock transcription factor 2  | <i>HSF2</i>     | −1.0091325 | ko03000   |
| inositol monophosphatase domain containing 1                                     | <i>IMPAD1</i>   | −1.0071035 | ko00562, ko00920, ko01100, ko01120, ko01130, ko04070  |

NA: not available; Log2 FC \*: Log2 FC (MCF-7-chlorophyllides/MDA-MB-231-chlorophyllides).

TOP2 A was upregulated in MCF-7 and MDA-MB-231 cells. TOP2A acted as a DNA replication- and cell division-regulating enzyme. The overexpression of TOP2A was reported in several human cancers, including breast cancer and hepatocellular carcinoma [74]. Also, high levels of expression of chromatin regulatory genes (e.g., TOP2A) increased DNA accessibility and then led to greater anthracycline benefit [75]. Amplification of the *MYC* oncogene was the most common abnormality in breast cancer cells, which is similar to the previous study [50]. We also observed that *Myc* oncogenes were upregulated in chlorophyllides composites-treated MDA-MB-231 cells.

Breast cancer is regarded as a heterogeneous disease characterized by molecular aberrations and varying histologic and biological features. Microarray-based gene expression profiling had a significant impact on the understanding of breast cancers. The molecular classification system and prognostic multigene classifiers by microarrays was developed [10]. For example, correlation was found between immunohistochemistry and gene profiling of breast cancer, especially basal-like breast carcinoma. The intrinsic 40-gene set was found to classify breast cancer subtype and genes expression differentiations by microarray [76]. In addition, the gene expression profiling from triple negative breast cancer (TNBC) patients by next generation sequencing assay targeted all coding regions of 229 common cancer-related genes [77]. Genetic alterations in TNBC by next-generation sequencing assays was successfully detected [78]. Nonetheless, the functional annotation of common or specific unigenes provided ample numbers of candidate genes and valuable information about biological features of chlorophyllides composites treatment in this study.

#### 4. Conclusions

Chlorophyllides composites could be mass manufactured from chlorophyll using chlorophyllase. In addition, chlorophyllides composites clearly exhibited amazing anti-cancer activities to breast cancer cell lines (MCF-7 or MDA-MB-231) [37]. To the best of our knowledge, this study is the first to evaluate the effects of chlorophyllides composites on MCF-7 and MDA-MB-231 cells by microarray profile. Moreover, it is also first to identify the global gene expression pattern from the chlorophyllides-treated group. Results indicated that 124 and 77 differentially expressed genes in MCF-7 cells and MDA-MB-231 cells after chlorophyllides composites treatment ( $A \geq 2$ -fold change) was evident. Among these, it is possible to highlight that the expression of *CCR1*, *STIM2*, *ETNK1*, *MAG1* and *TOP2A* were upregulated in both chlorophyllides composites treated-MCF-7 and MDA-MB-231 cells, indicating that chlorophyllides composites may specifically target or inhibit the activity of these genes. Altogether, these results provide valuable information on the molecular mechanisms induced by chlorophyllides composites in MCF-7 and MDA-MB-231 cells. The DEGs of *NLRC5*, *SLC7A7* and *PKN1* may be used as therapy targets that facilitate the development of botanical drugs.

**Supplementary Materials:** The following are available online at <https://www.mdpi.com/article/10.3390/molecules27123950/s1>, Figure S1: HPLC analysis profiles of chlorophyllides composites [37,38].

**Author Contributions:** Conceptualization, K.-S.H.; Formal analysis, T.-Y.H. and M.-H.T.; Project administration, C.-H.Y.; Supervision, J.-F.S.; Writing—original draft, Y.-T.W.; Writing—review & editing, O.B. All authors have read and agreed to the published version of the manuscript.

**Funding:** This work was supported by the grants of the Ministry of Science and Technology, Taiwan (MOST 107-2311-B-214-002, MOST 108-2311-B-214-001, MOST 109-2311-B-214-001, MOST 109-2622-B-214-001, MOST 110-2311-B-214-001 and MOST 110-2320-B-214-003) to Jei-Fu Shaw and Chih-Hui Yang. There was no additional external funding received for this study.

**Institutional Review Board Statement:** Not applicable.

**Informed Consent Statement:** Not applicable.

**Data Availability Statement:** Data is contained within the article or supplementary material.

**Conflicts of Interest:** The authors declare that there is no conflict of interest regarding the publication of this article.

**Sample Availability:** Samples of the compounds-chlorophyllides conposites are available from the author (Jei-Fu Shaw).

### Abbreviations

|           |   |
|-----------|---|
| (ANXA4)   | annexin A4  |
| (BP)      | biological process  |
| (CC)      | cellular component  |
| (CCR1)    | chemokine C-C motif receptor 1                                      |
| (TOP2A)   | DNA topoisomerase II alpha 170 kDa                                  |
| (ER)      | estrogen receptor   |
| (ETNK1)   | ethanolamine kinase 1   |
| (FC)      | fold change   |
| (HER2)    | human epidermal growth receptor 2                                   |
| (RAP2B)   | member of RAS oncogene family                                       |
| (MAGI1)   | membrane associated guanylate kinase WW and PDZ domain containing 1 |
| (MF)      | molecular function  |
| (NLRC5)   | NLR family CARD domain containing 5                                 |
| (SLC7A7)  | solute carrier family 7 membrane 7                                  |
| (STIM2)   | stromal interaction molecule 2                                      |
| (PR)      | progesterone receptor   |
| (PKN1)    | protein kinase N1   |
| (TNBC)    | triple negative breast cancer                                       |
| (RT-qPCR) | quantitative reverse transcription PCR                              |

### References

1. Siegel, R.L.; Miller, K.D.; Fuchs, H.E.; Jemal, A. Cancer Statistics, 2021. *CA A Cancer J. Clin.* **2021**, *71*, 7–33. [[CrossRef](#)] [[PubMed](#)]
2. McCann, K.E.; Hurvitz, S.A.; McAndrew, N. Advances in targeted therapies for triple-negative breast cancer. *Drugs* **2019**, *79*, 1217–1230. [[CrossRef](#)] [[PubMed](#)]
3. DeSantis, C.E.; Ma, J.; Gaudet, M.M.; Newman, L.A.; Miller, K.D.; Goding Sauer, A.; Jemal, A.; Siegel, R.L. Breast cancer statistics, 2019. *CA A Cancer J. Clin.* **2019**, *69*, 438–451. [[CrossRef](#)] [[PubMed](#)]
4. Reddy, T.P.; Rosato, R.R.; Li, X.; Moulder, S.; Piwnica-Worms, H.; Chang, J.C. A comprehensive overview of metaplastic breast cancer: Clinical features and molecular aberrations. *Breast Cancer Res.* **2020**, *22*, 121. [[CrossRef](#)] [[PubMed](#)]
5. Loibl, S.; Poortmans, P.; Morrow, M.; Denkert, C.; Curigliano, G. Breast cancer. *Lancet* **2021**, *10286*, 1750–1769. [[CrossRef](#)]
6. Comşa, Ş.; Cîmpean, A.M.; Raica, M. The Story of MCF-7 Breast Cancer Cell Line: 40 years of Experience in Research. *Anticancer Res.* **2015**, *35*, 3147.
7. Theodossiou, T.A.; Ali, M.; Grigalavicius, M.; Grallert, B.; Dillard, P.; Schink, K.O.; Olsen, C.E.; Wälchli, S.; Inderberg, E.M.; Kubin, A.; et al. Simultaneous defeat of MCF7 and MDA-MB-231 resistances by a hypericin PDT–tamoxifen hybrid therapy. *NPJ Breast Cancer* **2019**, *5*, 13. [[CrossRef](#)]
8. Yin, L.; Duan, J.J.; Bian, X.W.; Yu, S.C. Triple-negative breast cancer molecular subtyping and treatment progress. *Breast Cancer Res.* **2020**, *22*, 61. [[CrossRef](#)]
9. da Silva, J.L.; Cardoso Nunes, N.C.; Izetti, P.; de Mesquita, G.G.; de Melo, A.C. Triple negative breast cancer: A thorough review of biomarkers. *Crit. Rev. Oncol. Hematol.* **2020**, *145*, 102855. [[CrossRef](#)]
10. Reis-Filho, J.S.; Pusztai, L. Gene expression profiling in breast cancer: Classification, prognostication, and prediction. *Lancet* **2011**, *378*, 1812–1823. [[CrossRef](#)]
11. González-Martínez, S.; Pérez-Mies, B.; Carretero-Barrio, I.; Palacios-Berraquero, M.L.; Perez-García, J.; Cortés, J.; Palacios, J. Molecular Features of Metaplastic Breast Carcinoma: An Infrequent Subtype of Triple Negative Breast Carcinoma. *Cancers* **2020**, *12*, 1832. [[CrossRef](#)] [[PubMed](#)]
12. Waks, A.G.; Winer, E.P. Breast cancer treatment: A review. *JAMA* **2019**, *321*, 288–300. [[CrossRef](#)] [[PubMed](#)]
13. Montemurro, F.; Nuzzolese, I.; Ponzzone, R. Neoadjuvant or adjuvant chemotherapy in early breast cancer? *Expert Opin. Pharm.* **2020**, *21*, 1071–1082. [[CrossRef](#)]
14. Diaby, V.; Tawk, R.; Sanogo, V.; Xiao, H.; Montero, A.J. A review of systematic reviews of the cost-effectiveness of hormone therapy, chemotherapy, and targeted therapy for breast cancer. *Breast Cancer Res. Treat.* **2015**, *151*, 27–40. [[CrossRef](#)] [[PubMed](#)]
15. Shigematsu, H.; Fujisawa, T.; Shien, T.; Iwata, H. Omitting surgery for early breast cancer showing clinical complete response to primary systemic therapy. *Jpn. J. Clin. Oncol.* **2020**, *50*, 629–634. [[CrossRef](#)]

16. Recht, A.; McArthur, H.; Solin, L.J.; Tendulkar, R.; Whitley, A.; Giuliano, A. Contemporary guidelines in whole-breast irradiation: An alternative perspective. *Int. J. Radiat. Oncol. Biol. Phys.* **2019**, *104*, 567–573. [[CrossRef](#)]
17. Castaneda, S.A.; Strasser, J. Updates in the treatment of breast cancer with radiotherapy. *Surg. Oncol. Clin.* **2017**, *26*, 371–382. [[CrossRef](#)]
18. Lyseng-Williamson, K.A.; Fenton, C. Docetaxel: A review of its use in metastatic breast cancer. *Drugs* **2005**, *65*, 2513–2531. [[CrossRef](#)]
19. Willson, M.L.; Burke, L.; Ferguson, T.; Ghersi, D.; Nowak, A.K.; Wilcken, N. Taxanes for adjuvant treatment of early breast cancer. *Cochrane Database Syst. Rev.* **2019**, *9*, CD004421. [[CrossRef](#)]
20. Alqahtani, F.Y.; Aleanizy, F.S.; El Tahir, E.; Alkahtani, H.M.; AlQuadeib, B.T. Chapter Three—Paclitaxel. In *Profiles of Drug Substances, Excipients and Related Methodology*; Brittain, H.G., Ed.; Academic Press: Cambridge, MA, USA, 2019; Volume 44, pp. 205–238.
21. Gallego-Jara, J.; Lozano-Terol, G.; Sola-Martínez, R.A.; Cánovas-Díaz, M.; de Diego Puente, T. A compressive review about Taxol®: History and future challenges. *Molecules* **2020**, *25*, 5986. [[CrossRef](#)]
22. Dehelean, C.A.; Marcovici, I.; Soica, C.; Mioc, M.; Coricovac, D.; Iurciuc, S.; Cretu, O.M.; Pinzaru, I. Plant-derived anticancer compounds as new perspectives in drug discovery and alternative therapy. *Molecules* **2021**, *26*, 1109. [[CrossRef](#)] [[PubMed](#)]
23. Nacht, M.; Ferguson, A.T.; Zhang, W.; Petroziello, J.M.; Cook, B.P.; Gao, Y.H.; Maguire, S.; Riley, D.; Coppola, G.; Landes, G.M.; et al. Combining serial analysis of gene expression and array technologies to identify genes differentially expressed in breast cancer. *Cancer Res.* **1999**, *59*, 5464–5470.
24. Russo, G.; Zegar, C.; Giordano, A. Advantages and limitations of microarray technology in human cancer. *Oncogene* **2003**, *22*, 6497–6507. [[CrossRef](#)] [[PubMed](#)]
25. Rao, M.S.; Van Vleet, T.R.; Ciurlionis, R.; Buck, W.R.; Mittelstadt, S.W.; Blomme, E.A.G.; Liguori, M.J. Comparison of RNA-Seq and Microarray Gene Expression Platforms for the Toxicogenomic Evaluation of Liver From Short-Term Rat Toxicity Studies. *Front. Genet.* **2019**, *9*, 636. [[CrossRef](#)] [[PubMed](#)]
26. Januchowski, R.; Sterzyńska, K.; Zawierucha, P.; Ruciński, M.; Świerczewska, M.; Partyka, M.; Bednarek-Rajewska, K.; Brażert, M.; Nowicki, M.; Zabel, M.; et al. Microarray-based detection and expression analysis of new genes associated with drug resistance in ovarian cancer cell lines. *Oncotarget* **2017**, *8*, 49944–49958. [[CrossRef](#)]
27. Sandhu, R.; Parker, J.S.; Jones, W.D.; Livasy, C.A.; Coleman, W.B. Microarray-Based Gene Expression Profiling for Molecular Classification of Breast Cancer and Identification of New Targets for Therapy. *Lab. Med.* **2010**, *41*, 364–372. [[CrossRef](#)]
28. Si, W.; Shen, J.; Zheng, H.; Fan, W. The role and mechanisms of action of microRNAs in cancer drug resistance. *Clin. Epigenetics* **2019**, *11*, 25. [[CrossRef](#)]
29. Malvia, S.; Bagadi, S.A.R.; Pradhan, D.; Chintamani, C.; Bhatnagar, A.; Arora, D.; Sarin, R.; Saxena, S. Study of Gene Expression Profiles of Breast Cancers in Indian Women. *Sci. Rep.* **2019**, *9*, 10018. [[CrossRef](#)]
30. Glinsky, G.V.; Berezovska, O.; Glinskii, A.B. Microarray analysis identifies a death-from-cancer signature predicting therapy failure in patients with multiple types of cancer. *J. Clin. Investig.* **2005**, *115*, 1503–1521. [[CrossRef](#)]
31. Yoshimaru, T.; Nakamura, Y.; Katagiri, T. Functional genomics for breast cancer drug target discovery. *J. Hum. Genet.* **2021**, *66*, 927–935. [[CrossRef](#)]
32. Kim, G.-E.; Kim, N.I.; Lee, J.S.; Park, M.H.; Kang, K. Differentially Expressed Genes in Matched Normal, Cancer, and Lymph Node Metastases Predict Clinical Outcomes in Patients With Breast Cancer. *Appl. Immunohistochem. Mol. Morphol.* **2020**, *28*, 111. [[CrossRef](#)] [[PubMed](#)]
33. Kuo, W.-H.; Chang, Y.-Y.; Lai, L.-C.; Tsai, M.-H.; Hsiao, C.K.; Chang, K.-J.; Chuang, E.Y. Molecular Characteristics and Metastasis Predictor Genes of Triple-Negative Breast Cancer: A Clinical Study of Triple-Negative Breast Carcinomas. *PLoS ONE* **2012**, *7*, e45831. [[CrossRef](#)] [[PubMed](#)]
34. Bellon, J.R.; Burstein, H.J.; Frank, E.S.; Mittendorf, E.A.; King, T.A. Multidisciplinary considerations in the treatment of triple-negative breast cancer. *CA A Cancer J. Clin.* **2020**, *70*, 432–442. [[CrossRef](#)] [[PubMed](#)]
35. Sotiriou, C.; Pusztai, L. Gene-Expression Signatures in Breast Cancer. *New Engl. J. Med.* **2009**, *360*, 790–800. [[CrossRef](#)]
36. Hortobagyi, G.N. Treatment of Breast Cancer. *N. Engl. J. Med.* **1998**, *339*, 974–984. [[CrossRef](#)] [[PubMed](#)]
37. Wang, Y.T.; Yang, C.H.; Huang, T.Y.; Tai, M.H.; Sie, R.H.; Shaw, J.F. Cytotoxic effects of chlorophyllides in ethanol crude extracts from plant leaves. *Evid Based Complement Altern. Med.* **2019**, *2019*, 9494328. [[CrossRef](#)]
38. Hsiang, Y.P.; Wang, Y.T.; Huang, K.S.; Huang, T.Y.; Tai, M.H.; Lin, Y.M.; Yang, C.H.; Shaw, J.F. Facile production of chlorophyllides using recombinant CrCLH1 and their cytotoxicity towards multidrug resistant breast cancer cell lines. *PLoS ONE* **2021**, *16*, e0250565. [[CrossRef](#)]
39. Qin, H.; Li, S.; Li, D. An improved method for determining phytoplankton chlorophyll a concentration without filtration. *Hydrobiologia* **2013**, *707*, 81–95. [[CrossRef](#)]
40. Chou, Y.L.; Ko, C.Y.; Yen, C.C.; Chen, L.F.; Shaw, J.F. A novel recombinant chlorophyllase1 from *Chlamydomonas reinhardtii* for the production of chlorophyllide derivatives. *J. Agric. Food Chem.* **2015**, *63*, 9496–9503. [[CrossRef](#)]
41. Hummon, A.B.; Lim, S.R.; Difilippantonio, M.J.; Ried, T. Isolation and solubilization of proteins after TRIzol extraction of RNA and DNA from patient material following prolonged storage. *Biotechniques* **2007**, *42*, 467–472. [[CrossRef](#)]

42. Sheu, C.C.; Tsai, M.J.; Chen, F.W.; Chang, K.F.; Chang, W.A.; Chong, I.W.; Kuo, P.L.; Hsu, Y.L. Identification of novel genetic regulations associated with airway epithelial homeostasis using next-generation sequencing data and bioinformatics approaches. *Oncotarget* **2017**, *8*, 82674–82688. [[CrossRef](#)] [[PubMed](#)]
43. Livak, K.J.; Schmittgen, T.D. Analysis of relative gene expression data using real-time quantitative PCR and the 2<sup>(-Delta Delta C(T))</sup> Method. *Methods* **2001**, *25*, 402–408. [[CrossRef](#)]
44. Wang, Y.; Yu, J.; Cui, R.; Lin, J.; Ding, X. Curcumin in Treating Breast Cancer: A Review. *J. Lab. Autom.* **2016**, *21*, 723–731. [[CrossRef](#)] [[PubMed](#)]
45. Wang, X.; Yang, Y.; An, Y.; Fang, G. The mechanism of anticancer action and potential clinical use of kaempferol in the treatment of breast cancer. *Biomed. Pharm.* **2019**, *117*, 109086. [[CrossRef](#)] [[PubMed](#)]
46. Yin, R.; Li, T.; Tian, J.X.; Xi, P.; Liu, R.H. Ursolic acid, a potential anticancer compound for breast cancer therapy. *Crit. Rev. Food Sci. Nutr.* **2018**, *58*, 568–574. [[CrossRef](#)]
47. Ezzati, M.; Yousefi, B.; Velaei, K.; Safa, A. A review on anti-cancer properties of Quercetin in breast cancer. *Life Sci.* **2020**, *248*, 117463. [[CrossRef](#)]
48. Guo, W.; Xu, B.; Wang, X.; Zheng, B.; Du, J.; Liu, S. The Analysis of the Anti-Tumor Mechanism of Ursolic Acid Using Connectively Map Approach in Breast Cancer Cells Line MCF-7. *Cancer Manag. Res.* **2020**, *12*, 3469–3476. [[CrossRef](#)]
49. Bachmeier, B.E.; Mohrenz, I.V.; Mirisola, V.; Schleicher, E.; Romeo, F.; Höhneke, C.; Jochum, M.; Nerlich, A.G.; Pfeffer, U. Curcumin downregulates the inflammatory cytokines CXCL1 and -2 in breast cancer cells via NFkappaB. *Carcinogenesis* **2008**, *29*, 779–789. [[CrossRef](#)]
50. Li, W.; Liu, J.; Zhang, B.; Bie, Q.; Qian, H.; Xu, W. Transcriptome Analysis Reveals Key Genes and Pathways Associated with Metastasis in Breast Cancer. *OncoTargets Ther.* **2020**, *13*, 323–335. [[CrossRef](#)]
51. Sun, N.; Gao, P.; Li, Y.; Yan, Z.; Peng, Z.; Zhang, Y.; Han, F.; Qi, X. Screening and Identification of Key Common and Specific Genes and Their Prognostic Roles in Different Molecular Subtypes of Breast Cancer. *Front. Mol. Biosci.* **2021**, *8*, 619110. [[CrossRef](#)]
52. Kim, C.; Kim, B. Anti-Cancer Natural Products and Their Bioactive Compounds Inducing ER Stress-Mediated Apoptosis: A Review. *Nutrients* **2018**, *10*, 1021. [[CrossRef](#)] [[PubMed](#)]
53. Akram, I.G.; Georges, R.; Hielscher, T.; Adwan, H.; Berger, M.R. The chemokines CCR1 and CCRL2 have a role in colorectal cancer liver metastasis. *Tumor Biol.* **2016**, *37*, 2461–2471. [[CrossRef](#)] [[PubMed](#)]
54. Korbecki, J.; Kojder, K.; Barczak, K.; Simińska, D.; Gutowska, I.; Chlubek, D.; Baranowska-Bosiacka, I. Hypoxia alters the expression of CC chemokines and CC chemokine receptors in a tumor—a literature review. *Int. J. Mol. Sci.* **2020**, *21*, 5647. [[CrossRef](#)] [[PubMed](#)]
55. Krishnan, V.; Tallapragada, S.; Schaar, B.; Kamat, K.; Chanana, A.M.; Zhang, Y.; Patel, S.; Parkash, V.; Rinker-Schaeffer, C.; Folkins, A.K.; et al. Omental macrophages secrete chemokine ligands that promote ovarian cancer colonization of the omentum via CCR1. *Commun. Biol.* **2020**, *3*, 524. [[CrossRef](#)]
56. Shin, S.Y.; Lee, D.H.; Lee, J.; Choi, C.; Kim, J.Y.; Nam, J.S.; Lim, Y.; Lee, Y.H. C-C motif chemokine receptor 1 (CCR1) is a target of the EGF-AKT-mTOR-STAT3 signaling axis in breast cancer cells. *Oncotarget* **2017**, *8*, 94591–94605. [[CrossRef](#)]
57. Liu, F.; Wu, H. CC chemokine receptors in lung adenocarcinoma: The inflammation-related prognostic biomarkers and immunotherapeutic targets. *J. Inflamm. Res.* **2021**, *14*, 267–285. [[CrossRef](#)]
58. Emrich, S.M.; Yoast, R.E.; Xin, P.; Zhang, X.; Pathak, T.; Nwokonko, R.; Gueguinou, M.F.; Subedi, K.P.; Zhou, Y.; Ambudkar, I.S.; et al. Cross-talk between N-terminal and C-terminal domains in stromal interaction molecule 2 (STIM2) determines enhanced STIM2 sensitivity. *J. Biol. Chem.* **2019**, *294*, 6318–6332. [[CrossRef](#)]
59. Novello, M.J.; Zhu, J.; Feng, Q.; Ikura, M.; Stathopoulos, P.B. Structural elements of stromal interaction molecule function. *Cell Calcium* **2018**, *73*, 88–94. [[CrossRef](#)]
60. Nelson, H.A.; Roe, M.W. Molecular physiology and pathophysiology of stromal interaction molecules. *Exp. Biol. Med.* **2018**, *243*, 451–472. [[CrossRef](#)]
61. Berna-Erro, A.; Jardin, I.; Salido, G.M.; Rosado, J.A. Role of STIM2 in cell function and physiopathology. *J. Physiol.* **2017**, *595*, 3111–3128. [[CrossRef](#)]
62. López, E.; Salido, G.M.; Rosado, J.A.; Berna-Erro, A. Unraveling STIM2 function. *J. Physiol. Biochem.* **2012**, *68*, 619–633. [[CrossRef](#)] [[PubMed](#)]
63. Lasho, T.L.; Finke, C.M.; Zblewski, D.; Patnaik, M.; Ketterling, R.P.; Chen, D.; Hanson, C.A.; Tefferi, A.; Pardanani, A. Novel recurrent mutations in ethanolamine kinase 1 (ETNK1) gene in systemic mastocytosis with eosinophilia and chronic myelomonocytic leukemia. *Blood Cancer J.* **2015**, *5*, e275. [[CrossRef](#)] [[PubMed](#)]
64. Fontana, D.; Mauri, M.; Renso, R.; Docci, M.; Crespiatico, I.; Røst, L.M.; Jang, M.; Niro, A.; D’Aliberti, D.; Massimino, L.; et al. ETNK1 mutations induce a mutator phenotype that can be reverted with phosphoethanolamine. *Nat. Commun.* **2020**, *11*, 5938. [[CrossRef](#)] [[PubMed](#)]
65. Qu, D.; Huang, H.; Di, J.; Gao, K.; Lu, Z.; Zheng, J. Structure, functional regulation and signaling properties of Rap2B. *Oncol. Lett.* **2016**, *11*, 2339–2346. [[CrossRef](#)] [[PubMed](#)]
66. Li, Z.Y.; Li, X.H.; Tian, G.W.; Zhang, D.Y.; Gao, H.; Wang, Z.Y. MAGI1 inhibits the proliferation, migration and invasion of glioma cells. *OncoTargets Ther.* **2019**, *12*, 11281–11290. [[CrossRef](#)] [[PubMed](#)]
67. Feng, X.; Jia, S.; Martin, T.A.; Jiang, W.G. Regulation and involvement in cancer and pathological conditions of MAGI1, a tight junction protein. *Anticancer Res.* **2014**, *34*, 3251–3256. [[PubMed](#)]

68. Shukla, A.; Cloutier, M.; Appiya Santharam, M.; Ramanathan, S.; Ilangumaran, S. The MHC Class-I Transactivator NLRC5: Implications to Cancer Immunology and Potential Applications to Cancer Immunotherapy. *Int. J. Mol. Sci.* **2021**, *22*, 1964. [[CrossRef](#)]
69. Cho, S.X.; Vijayan, S.; Yoo, J.S.; Watanabe, T.; Ouda, R.; An, N.; Kobayashi, K.S. MHC class I transactivator NLRC5 in host immunity, cancer and beyond. *Immunology* **2021**, *162*, 252–261. [[CrossRef](#)]
70. Noguchi, A.; Takahashi, T. Overview of symptoms and treatment for lysinuric protein intolerance. *J. Hum. Genet.* **2019**, *64*, 849–858. [[CrossRef](#)]
71. Bodoy, S.; Sotillo, F.; Espino-Guarch, M.; Sperandeo, M.P.; Ormazabal, A.; Zorzano, A.; Sebastio, G.; Artuch, R.; Palacín, M. Inducible Slc7a7 knockout mouse model recapitulates lysinuric protein intolerance disease. *Int. J. Mol. Sci.* **2019**, *20*, 5294. [[CrossRef](#)]
72. Zeng, R.; Wang, Z.; Li, X.; Chen, Y.; Yang, S.; Dong, J. Cyclin-dependent kinase 1-mediated phosphorylation of protein kinase N1 promotes anchorage-independent growth and migration. *Cell. Signal.* **2020**, *69*, 109546. [[CrossRef](#)] [[PubMed](#)]
73. Venkadakrishnan, V.B.; DePriest, A.D.; Kumari, S.; Senapati, D.; Ben-Salem, S.; Su, Y.; Mudduluru, G.; Hu, Q.; Cortes, E.; Pop, E.; et al. Protein Kinase N1 control of androgen-responsive serum response factor action provides rationale for novel prostate cancer treatment strategy. *Oncogene* **2019**, *38*, 4496–4511. [[CrossRef](#)] [[PubMed](#)]
74. Cai, H.; Shao, B.; Zhou, Y.; Chen, Z. High expression of TOP2A in hepatocellular carcinoma is associated with disease progression and poor prognosis. *Oncol. Lett.* **2020**, *20*, 232. [[CrossRef](#)] [[PubMed](#)]
75. Seoane, J.A.; Kirkland, J.G.; Caswell-Jin, J.L.; Crabtree, G.R.; Curtis, C. Chromatin regulators mediate anthracycline sensitivity in breast cancer. *Nat. Med.* **2019**, *25*, 1721–1727. [[CrossRef](#)]
76. Wu, Y.M.; Hu, W.; Wang, Y.; Wang, N.; Gao, L.; Chen, Z.Z.; Zheng, W.Q. Exploring novel targets of basal-like breast carcinoma by comparative gene profiling and mechanism analysis. *Breast Cancer Res. Treat.* **2013**, *141*, 23–32. [[CrossRef](#)]
77. Weisman, P.S.; Ng, C.K.Y.; Brogi, E.; Eisenberg, R.E.; Won, H.H.; Piscuoglio, S.; De Filippo, M.R.; Ioris, R.; Akram, M.; Norton, L.; et al. Genetic alterations of triple negative breast cancer by targeted next-generation sequencing and correlation with tumor morphology. *Mod. Pathol.* **2016**, *29*, 476–488. [[CrossRef](#)]
78. Dillon, J.L.; Mockus, S.M.; Ananda, G.; Spottlow, V.; Wells, W.A.; Tsongalis, G.J.; Marotti, J.D. Somatic gene mutation analysis of triple negative breast cancers. *Breast* **2016**, *29*, 202–207. [[CrossRef](#)]